A method for modulation transfer function determination from edge profiles with correction for finite-element differentiation

I. A. Cunningham[a] and A. Fenster
Department of Medical Biophysics and the R. B. Holmes Radiological Research Laboratories, University of Toronto, Toronto, Ontario, Canada M4X 1K9

(Received 17 December 1986; accepted for publication 31 March 1987)

In this paper we describe a technique for determining the modulation transfer function (MTF) of an imaging system from an experimentally obtained edge profile. The technique includes an exact correction for the frequency passband of the finite-element differentiation required to obtain the line spread function from the edge spread function. This correction has been ignored by investigators in the past and is required whenever finite-element differentiation is used rather than analytic differentiation of a model fitted to the edge response data. The magnitude of the MTF correction is $\sim 11\%$ at $f = f_c/2$ and $\sim 57\%$ at $f = f_c$, where $f_c = f_s/2$ is the maximum frequency reproducible without aliasing with a sampling rate of f_s. The correction is performed in the spatial frequency domain by multiplying the uncorrected MTF by $1/\mathrm{sinc}(\pi f/2f_c)$. A computer simulation is presented to demonstrate the effect and the correction procedure. An experimental MTF of an x-ray image intensifier system obtained using this technique is found to be consistent with an MTF obtained using a bar pattern test phantom.

Key words: modulation transfer function (MTF), edge spread function (ESF), line spread function (LSF), finite-element differentiation

I. INTRODUCTION

The modulation transfer function (MTF) has been used widely to characterize the spatial frequency response (spatial resolution) of many kinds of imaging systems. It can be used with systems that are linear and spatially invariant.[1] While these conditions are not always well satisfied, the approach has been widely accepted and the MTF's obtained usually provide a useful measure of system performance for comparisons and characterization.

Many different techniques have been used to obtain the MTF, and generally involve either recording an image on film and subsequently sampling it digitally with a scanning microdensitometer, or obtaining a digital image directly with a digital imaging system. For example, bar pattern resolution test phantoms can be imaged and the MTF calculated from the observed system response to the square-wave pattern.[2–4] The MTF can also be calculated from the system line spread function[5] (LSF), which can be determined directly by imaging fine wires[6] or narrow slits.[7,8] Care must be taken to avoid problems associated with aliasing[6,8,9] when performing these measurements. Alternatively, the LSF can be determined from the system edge spread function (ESF). The ESF is obtained by imaging the edge of an opaque surface, and is differentiated to generate the LSF. This technique is frequently used to determine the MTF of computed tomographic systems.[10–12]

The differentiation of the ESF can be done in a number of ways and is the subject of this paper. Some investigators have fitted a model such as the error function to the ESF and differentiated analytically producing a Gaussian-shaped LSF.[12] Alternatively, some have fitted the ESF data with an assumed shape or function locally (e.g., linear, cubic spline) and differentiated.[10,13] Those who have not wanted to force their data to an assumed model have performed the differentiation numerically using a finite-element technique. However, a problem arises with the finite-element technique due to the spacing of the sampled data if the system is not sufficiently oversampled. This results from the fact that one approximates the true derivative of the ESF at each position by the slope between neighboring pixels. It is shown here that the resulting estimated MTF contains an error which remains unimportant only if the sampling rate is approximately $4\times$ the Nyquist frequency or greater.

Although these considerations are not novel, it seems this problem has been largely ignored in the medical imaging literature.[14–18] Judy[10] is one of the few who acknowledge the problem but notes that it is unimportant in his case. It can be made to be unimportant for those who digitize films by choosing a sufficiently large sampling frequency, however digital radiographic imaging systems generally have a fixed sampling frequency, and a correction for this effect is necessary.

This paper reviews the theory of determining the MTF from the ESF using a Fourier domain analysis in order to describe the difference in the spatial frequency response in finite-element differentiation from that of analytic differentiation. A simple but exact procedure is then given to correct for this frequency response difference. Results of a computer simulation and an experimental MTF determination using an x-ray image intensifier (XRII) system are presented, and a comparison is made with the MTF determined from a bar pattern image. It should be noted that although the correction procedure is applied here to an XRII system, it is equally applicable to the MTF determination of any imaging system if finite-element differentiation is used.

In this paper extensive use is made of the convolution theorem,[19] which states that convolution in the spatial domain corresponds to multiplication in the frequency do-

 0094-2405/87/040533-05$01.20

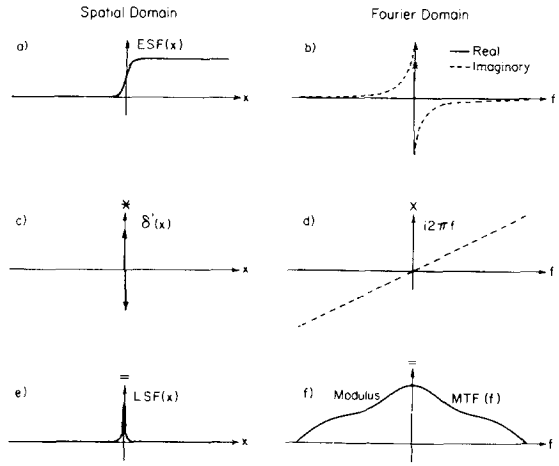

FIG. 1. The procedure for determining the MTF from the ESF of a nonsampled system consists of steps that can be presented in the spatial domain (left-hand side) or in the spatial frequency domain (right-hand side). The analytic differentiation step is shown in (c) as a convolution with $\delta'(x)$, the first derivative of the impulse function $\delta(x)$. Its frequency passband is shown in (d). The resulting correct MTF is shown in (f).

main, and vice versa. It is also important to remember that only the even (cosine) component of an arbitrary function can be correctly reproduced when sampled at the Nyquist frequency. The odd (sine) component must be sampled at a slightly greater frequency, as described by Bracewell.[20] This is generally not a problem if there is no aliasing in the ESF measurement.

II. THEORY

The process of calculating the MTF from the ESF is shown schematically for a hypothetical analytic system in Fig. 1, and for a sampled system in Fig. 2. The curves on the left-hand side of each figure, represent functions in the spatial domain, and the curves on the right-hand side represent the corresponding Fourier transforms in the spatial frequency domain. It is assumed there is no aliasing in the sampled system. The effect of the pixel aperture width on the MTF is not considered separately as it is considered an integral part of the system MTF. The determination of the MTF from the ESF for the analytic case is described first, followed by a similar description for the sampled case.

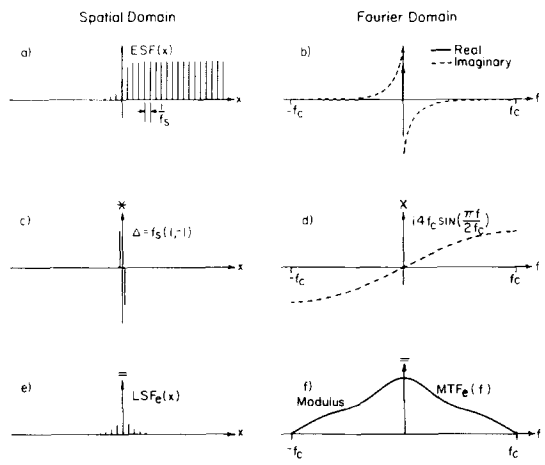

FIG. 2. The procedure for determining the MTF of a sampled system requires finite-element differentiation, shown in (c) as a convolution with Δ, the finite-element difference operator. The frequency passband of this operation is shown in (d) and differs to that of analytic differentiation shown in Fig. 1(d). The resulting distorted MTF is shown in (f).

The system response to an edge profile of x-ray intensities (ESF) is shown in Fig. 1(a) and its Fourier transform in Fig. 1(b). The LSF [Fig. 1(e)] is obtained by differentiating the ESF. This is done analytically in the spatial domain as expressed by

$$\mathrm{LSF}(x) = \frac{d}{dx}\,\mathrm{ESF}(x). \tag{1}$$

Following Bracewell,[21] the differentiation can also be expressed as a convolution operation given by

$$\mathrm{LSF}(x) = \mathrm{ESF}(x) * \delta'(x), \tag{2}$$

where * represents the one-dimensional convolution operation and $\delta'(x)$ is the first derivative of the impulse function $\delta(x)$. This differentiation step is shown graphically in Fig. 1(c). The MTF is the normalized modulus of the Fourier transform of the LSF as shown in Fig. 1(f). An equivalent way of obtaining the same result is by multiplying the transform of the ESF by the transform of $\delta'(x)$, $i2\pi f$, as shown in Fig. 1(d). In both cases the result is exact.

The process for determining the MTF of a sampled system is shown in Fig. 2. Figure 2(a) shows the edge profile obtained with a system that samples the profile in Fig. 1(a) at a frequency f_s. The Fourier transform of this function is shown in Fig. 2(b) and repeats at multiples of f_s (not shown). All frequencies up to the cutoff frequency f_c can be accurately reproduced without aliasing, where $f_c = f_s/2$. The differentiation is performed in the spatial domain using finite-element differences so that

$$\mathrm{LSF}(x_j) = [1/(x_j - x_{j-1})][\mathrm{ESF}(x_j) - \mathrm{ESF}(x_{j-1})], \tag{3}$$

where j represents the sample number. Again following Bracewell,[21] this operation can be expressed as a convolution with the finite-difference operator as

$$\mathrm{LSF}(x) = \mathrm{ESF}(x) * \Delta, \tag{4}$$

where Δ represents the two-element kernal with values $f_s(1, -1)$ as shown in Fig. 2(c). The result [Fig. 2(e)] is an estimate of the true LSF and is converted into $\mathrm{MTF}_e(f)$, an estimate of the true MTF, with the fast Fourier transform[22] [Fig. 2(f)].

The frequency response of the finite-element method can be determined from the Fourier domain analysis. The Fourier transform of Δ is $i4f_c \sin(\pi f/2f_c)$ and hence differentiation in the spatial domain corresponds to multiplication by this function in the frequency domain as shown in Fig. 2(d). The result, $\mathrm{MTF}_e(f)$, is periodic and repeats at multiples of f_s. The shape of $\mathrm{MTF}_e(f)$ is different from that of the analytic $\mathrm{MTF}(f)$ [Fig. 1(f)] because the frequency response of the finite-element differentiation [Fig. 2(d)] is different from that of analytic differentiation [Fig. 1(d)]. The ratio of the true MTF to the estimated MTF is given by

$$\alpha(f) = \mathrm{MTF}(f)/\mathrm{MTF}_e(f)$$
$$= \frac{i2\pi f}{i4f_c \sin(\pi f/2f_c)} = \frac{1}{\mathrm{sinc}\,(\pi f/2f_c)}. \quad (5)$$

The true MTF(f) can, therefore, be recovered in the sampled case by multiplication with the correction function $\alpha(f)$ giving

$$\mathrm{MTF}(f) = \mathrm{MTF}_e(f) \times \alpha(f). \quad (6)$$

This correction function is plotted in Fig. 3. It is continuous and well behaved with a value between 1 and $\pi/2$ (~ 1.57) only for $|f| \leqslant f_c$.

III. COMPUTER SIMULATION

A computer simulation is used to demonstrate this differentiation artifact and the use of the correction function under ideal noise-free conditions. To do this, it is more convenient to use the function sinc(x) as the ESF rather than a more realistic edge profile, as sinc(x) is band limited and its transform is a rectangle which allows the artifact to be readily recognized in the Fourier domain. If the sinc(x) function [Fig. 4(a)] is sampled with a spacing of $1/f_s = 3\pi/2$ rad, the cutoff frequency f_c is given by $f_c = f_s/2 = 1/3\pi$, which is greater than the maximum frequency component in sinc(x), f_m, where $f_m = 1/2\pi = 0.75f_c$. There is therefore no aliasing in the sampled ESF. The ESF is differentiated by convolving with Δ [Fig. 4(c)] and the resulting LSF is shown in Fig. 4(e). The effect of finite-element differentiation is apparent in the sloped sections of the transform in Fig. 4(f). These would be straight for analytic differentiation, but here are found to curve downward. This artifact can be corrected with Eq. (6) as shown in Fig. 4(h). The result, shown in Fig. 4(j), is the true transform of d/dx sinc(x). In this example, the maximum error before correction is $\sim 28\%$ at $f = 0.75f_c$.

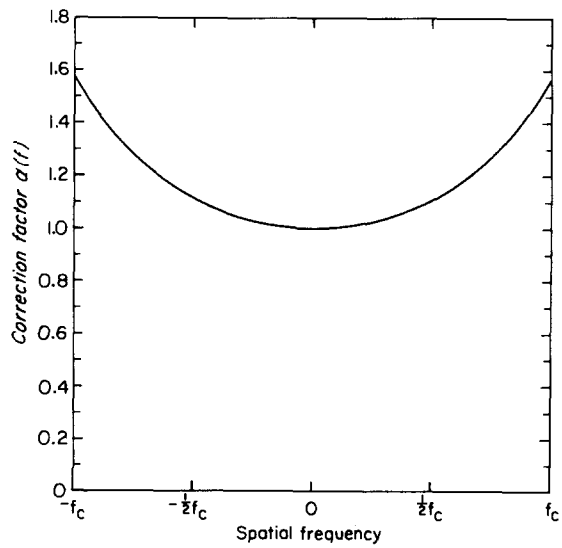

FIG. 3. The MTF can be corrected for the finite-differentiation step with the functions shown here. The function has the form $1/\mathrm{sinc}(\pi f/2f_c)$ and values of ~ 1.11 and ~ 1.57 at $f = f_c/2$ and $f = f_c$, respectively, where f_c is one-half of the sampling frequency.

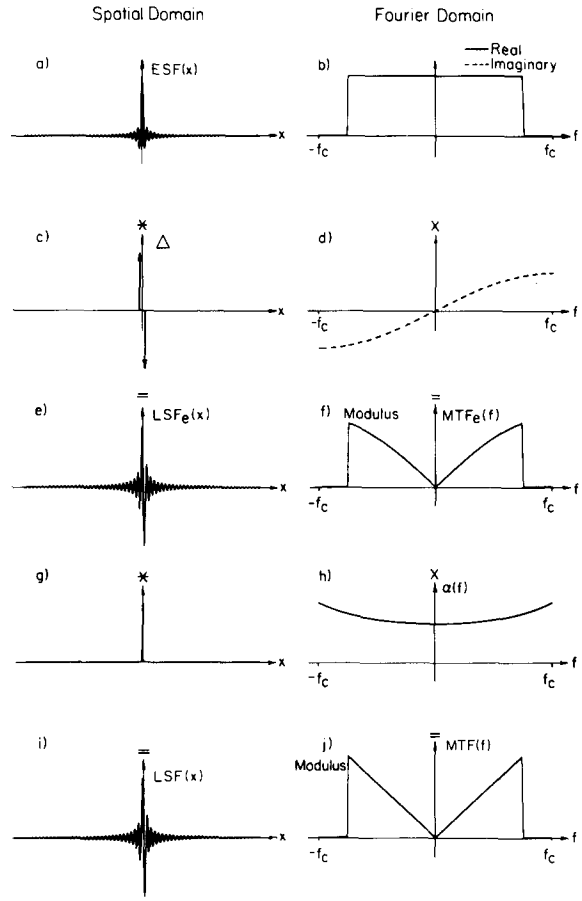

FIG. 4. A computer simulation demonstrates the artifact and the correction procedure. The ESF is the sinc(x) function in (a) sampled at a spacing of $3\pi/2$ rad. The ESF is differentiated by convolving with Δ in (c) to produce the estimate $\mathrm{LSF}_e(x)$ in (e). This is transformed with the FFT to produce the estimate $\mathrm{MTF}_e(x)$ in (f). Note the sloped sections of (f) are not straight as desired, but curve downward. The $\mathrm{MTF}_e(f)$ is multiplied by the correction function $\alpha(f) = 1/\mathrm{sinc}(\pi f/2f_c)$ in (h) to generate the true MTF(f) in (j) which has the expected straight sloped sections. The functions ESF(x), $\mathrm{LSF}_e(x)$, and LSF(x) are drawn as continuous functions for clarity.

It should be noted that ESF(x) [Fig. 4(a)] and $\mathrm{LSF}_e(x)$ [Fig. 4(e)] were modulated by the Hanning filter[22] before the fast Fourier transform (FFT) was calculated. This reduces side lobes and ringing in the transform at the expense of a slight blurring of the MTF(f) in the Fourier domain. The extent of the blurring is approximately the width of one element in the discrete Fourier transform. In the experimental example described in Sec. IV, this corresponds to approximately 0.009 cycles/mm. In addition, ESF(x), $\mathrm{LSF}_e(x)$, and LSF(x) in Fig. 4 are drawn as continuous functions, rather than sampled functions, for clarity.

IV. EXPERIMENTAL MTF DETERMINATION

The MTF of a prototype digital XRII system[23] was determined with this technique and compared with the MTF obtained from a bar pattern determination. The system consists of a Thomson CSF 9 in./6 in. XRII operated in the 9-in. mode and optically coupled through a slit assembly to a 1024-element linear photodiode array. The slit, located in a focused image plane, selects a single line of the image across

the central diameter of the XRII. This line had a width corresponding to 0.5 mm at the input phosphor with a pixel spacing of 0.23 mm. The diode array signal was digitized with a 12-bit linear analog-to-digital converter and stored in computer memory. No nonlinearity corrections are required.

The scatter rejection grid was removed and a 3-mm-thick lead plate was used to cover one-half of the input phosphor. The plate had a very smooth and square edge that was precisely aligned along the central axis of the XRII orthogonal to the slit. The ESF was obtained using an 80-kVp x-ray beam (filtered with 1.5 mm added Al only) and normalized to a scan obtained without the lead plate [Fig. 5(a)]. The method illustrated in Fig. 3 was used to calculate the MTF. Figure 6 shows the experimental MTF's obtained both with and without the artifact correction. It is apparent that the correction has a significant effect on the value of the MTF and is therefore required for a precise determination of the

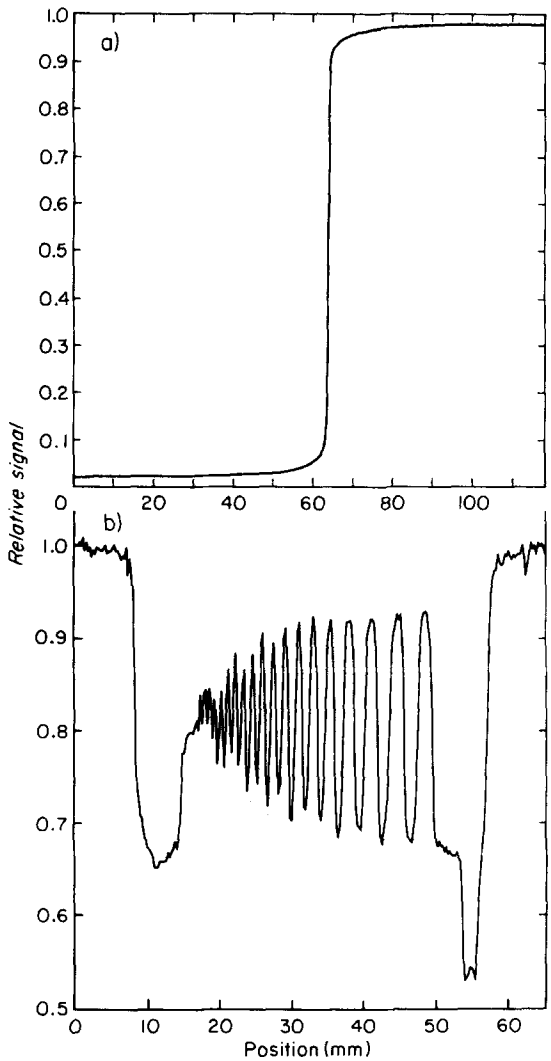

FIG. 5. (a) The experimental edge profile (ESF) used to determine the MTF which consists of 512 samples with a spacing of 0.23 mm. The MTF was also obtained from an image of a bar pattern for comparison. (b) Part of one scan line through the bar pattern.

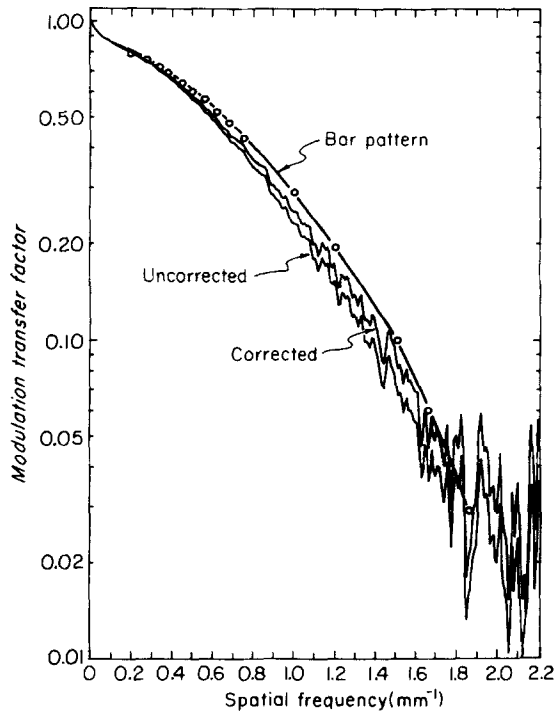

FIG. 6. Results of an experimental comparison of the uncorrected and corrected MTF's with the MTF obtained using the bar pattern technique. The two techniques give consistent results although the bar pattern result is slightly greater. This is due in part to the normalization which is necessarily done at a frequency greater than zero.

MTF. The error is greatest near the cutoff frequency (~ 2.2 mm^{-1}) and becomes insignificant below approximately $f_c/4$ (~ 0.5 mm^{-1}).

The MTF determined from a resolution test bar pattern (Type 10) obtained under the same radiological conditions is shown for comparison in Fig. 6. The harmonic frequency response was determined from the square-wave response using the method of Coltmann.[3,4] Sampling phase effects due to the position of the bar pattern with respect to the pixel positions were avoided by imaging the bar pattern at a small angle to the image scan lines. The maximum modulation in all scan lines at each square-wave frequency was used and the result normalized to unity in an 8-mm-wide region of the bar pattern. Figure 5(b) shows part of one of the scan lines. The lowest frequency (0.25 lp/mm) is at the 45-mm position and the highest frequency (approximately 2.0 lp/mm) is at the 17-mm position.

The bar pattern result and the corrected ESF result agree within a few percent, although the bar pattern result tends to be slightly greater. This is anticipated as the bar pattern amplitudes were normalized in a region only 8 mm wide on the pattern. This is equivalent to normalizing the bar pattern MTF to unity at a frequency greater than zero, which produces an MTF that is slightly greater than the actual MTF. The MTF obtained from the ESF is normalized in a 115-mm region (one-half of the input phosphor) which corresponds to a much lower frequency. It is clear however, that the correction for finite-element differentiation produces a result that is consistent with the bar pattern method.

V. CONCLUSION

A technique has been presented to determine the system MTF from an edge profile that incorporates a correction to the MTF for the frequency response of finite-element differentiation. The correction is performed by multiplying the uncorrected MTF(f) by $1/\mathrm{sinc}(\pi f/2f_c)$, where f_c is one-half of the sampling frequency. It constitutes an 11% correction at $f=f_c/2$ and 57% at $f=f_c$. The technique was described theoretically and illustrated with a computer simulation. An experimental MTF obtained with this technique was demonstrated to be consistent with the MTF obtained using a bar pattern technique on an x-ray image intensifier system.

ACKNOWLEDGMENTS

The authors would like to acknowledge Dr. J. A. Rowlands, Dr. M. J. Yaffe, Dr. P. C. Johns, R. N. Nishikawa, C. B. Caldwell, P. Munro, and N. Cardinal for their helpful comments and suggestions on this work. The financial assistance of the Medical Research Council of Canada, The Ontario Cancer Treatment and Research Foundation, and the National Cancer Institute of Canada is acknowledged. Dr. Ian A. Cunningham acknowledges the support of an Ontario Graduate Scholarship and Dr. A. Fenster acknowledges the financial support of the Health Research Personnel Development Program of the Ontario Ministry of Health.

[a] Address correspondence to: Dr. I. A. Cunningham, Department of Medical Biophysics & the R. B. Holmes Radiological Research Laboratories, University of Toronto, 500 Sherbourne Street, Toronto, Ontario, Canada M4X 1K9.

[1] C. E. Metz and K. Doi, Phys. Med. Biol. **24**, 1079 (1979).
[2] G. T. Barnes, in *The Physics of Medical Imaging: Recording System Measurements and Techniques*, edited by A. G. Haus (American Institute of Physics, New York, 1979).
[3] J. W. Coltmann, J. Opt. Soc. Am. **44**, 468 (1954).
[4] K. Rossmann, Radiology **93**, 257 (1969).
[5] H. H. Barrett and W. Swindell, *Radiological Imaging* (Academic, New York, 1981).
[6] R. A. Sones and G. T. Barnes, Med. Phys. **11**, 166 (1984).
[7] K. Doi, G. Holje, L. N. Loo, H. P. Chan, J. M. Sandrik, R. J. Jennings, and R. F. Wagner, "MTF's and Wiener Spectra of Radiological Screen–Film Systems," Bureau of Radiological Health Publ. (FDA) 82–8187, Rockville, MD (1982).
[8] H. Fujita, K. Doi, and M. L. Giger, Med. Phys. **12**, 713 (1985).
[9] R. T. Droege and M. S. Rzeszotarski, Med. Phys. **12**, 721 (1985).
[10] P. F. Judy, Med. Phys. **3**, 233 (1976).
[11] S. M. Bentzen, Med. Phys. **10**, 579 (1983).
[12] E. L. Nickoloff and R. Riley, Med. Phys. **12**, 437 (1985).
[13] K. W. Logan, K. A. Hickey, and S. R. Bull, Med. Phys. **10**, 361 (1983).
[14] R. A. Jones, Photogr. Sci. Eng. **11**, 102 (1967).
[15] *Physical Aspects of Medical Imaging*, edited by B. M. Moores, R. P. Parker, and B. R. Pullant (Wiley, Toronto, 1981).
[16] P. J. Bjorkholm, M. Annis, and E. E. Frederick, Proc. SPIE **233**, 137 (1980).
[17] R. M. Harrison and C. J. Kotre, Phys. Med. Biol. **31**, 515 (1986).
[18] J. C. Dainty and R. Shaw, *Image Science* (Academic, New York, 1974).
[19] R. N. Bracewell, *The Fourier Transform and its Applications*, 2nd ed. (McGraw–Hill, Toronto, 1978), p. 108.
[20] R. N. Bracewell, in Ref. 19, p. 194.
[21] R. N. Bracewell, in Ref. 19, p. 80.
[22] E. O. Brigham, *The Fast Fourier Transform* (Prentice–Hall, Toronto, 1974).
[23] I. A. Cunningham and A. Fenster, Med. Phys. **11**, 303 (1984).